Theoretical study of the structure of silver clusters

René Fournier[a)]
Department of Chemistry, York University, Toronto, Ontario M3J 1P3, Canada

(Received 18 September 2000; accepted 11 May 2001)

Neutral silver cluster isomers Ag_n ($n=2$ to 12) were studied by Kohn–Sham density functional theory. There is a strong even-odd oscillation in cluster stability due to spin subshell closing. Nearest-neighbor interatomic distances do not evolve continuously from the diatomic (2.53 Å) to the bulk (2.89 Å). After adding an empirical correction to the calculated values, we estimate that they are always near 2.68 Å for $3 \leqslant n \leqslant 6$, and near 2.74 Å for $7 \leqslant n \leqslant 12$. We find several low-energy isomers at all cluster sizes larger than seven atoms with one exception: Ag_{10} has a D_{2d} twinned pentagonal bipyramid isomer predicted to be 0.20 eV more stable than any other isomer. The ellipsoidal jellium model predicts rather well the shapes of stable silver clusters. Other models (extended Hückel, empirical potential) fail to reproduce the energy ordering of cluster isomers. The structural attributes of low-energy silver cluster isomers Ag_n ($n \geqslant 7$) are, in decreasing order of importance: a high mean coordination; a shape that conforms to the ellipsoidal jellium model; and uniformity in atomic coordinations. © *2001 American Institute of Physics.*
[DOI: 10.1063/1.1383288]

I. INTRODUCTION

There is continued interest in making and studying small atomic clusters. Many series of elemental clusters have been characterized in detail with a variety of experimental techniques. Properties that have been measured include: binding energies;[1,2] ion mobilities;[3–5] ionization potentials,[6,7] and more generally, electron binding energies;[8,9] magnetic moments;[10] electron spin densities;[11] UV-visible photoabsorption spectra;[12] vibrational modes characterized by Raman;[13,14] infra-red photodissociation;[12,15,16] and zero electron kinetic energy (ZEKE) spectroscopy;[17] and chemical reactivity towards small molecules.[18–20] Cluster properties vary with size and differ, sometimes dramatically, from those of the bulk,[6,10,21] but it is very hard to organize and understand the data accumulated about clusters without knowing their *geometrical structure*, as was pointed out many times (see, for example, Ref. 20). Structure is the basic model chemists use, yet very little is known about the structure of clusters in general. Elucidating the structure of atomic clusters is a challenging problem that requires piecing together informations from different experiments and theory. There are only a few elements for which we currently have reliable structural information over a significant size range: carbon,[22,23] silicon,[5,14] and, to a lesser degree, niobium[24] and silver (see the following). Indirect information about the structure of many clusters has been derived from adsorption experiments[20,25,26] (for Fe, Co, and Ni), and ion mobilities.[27]

Silver clusters are particularly interesting for a number of reasons. First, silver clusters and small particles have practical importance because of their role in photography,[28] in catalysis,[15] and their potential use in new electronic materials.[29] Also, the enhanced Raman effect observed for adsorbates on silver surfaces seems to have a cluster counterpart.[30] Second, the geometric structures of clusters of silver are among the best known after those of carbon and silicon. The triatomic has a D_{3h} ground state geometry which undergoes Jahn–Teller (JT) distortion leading to three equivalent C_{2v} obtuse isosceles triangle minima;[31–33] Ag_4 is a D_{2h} symmetry planar rhombus;[34] Ag_5 is a C_{2v} planar trapezoid;[35] two isomers of Ag_7 have been identified, a C_{3v} tricapped tetrahedron[36] and a D_{5h} pentagonal bipyramid;[37,38] and there have been tentative structural assignments for Ag_n ($n \leqslant 9$).[39] Third, although the structure of Ag_3, Ag_4, Ag_5 and Ag_7 are fairly well established, *structureless* theoretical models that ignore the precise positions of nuclei reproduce quite well the size variation of the stabilities and ionization potentials of group IA and IB clusters.[40] One of them, the ellipsoidal jellium model (EJM), gives predictions of the shape of coinage (Cu, Ag, Au) and alkali metal clusters.[41] This raises a number of questions. *Are silver clusters nonrigid*? This is a difficult question[42] which we cannot address satisfactorily by fixed geometry KS-DFT calculations. However, our calculations suggest that Ag_8, Ag_9, and possibly Ag_{12}, could be nonrigid at room temperature (208 cm^{-1}) if we consider the magnitudes of the lowest harmonic frequencies (20 to 50 cm^{-1}), and the mean frequency (120 cm^{-1}) in relation to the energy separation between the most stable isomers (150 to 600 cm^{-1}). *Do many isomers coexist at larger cluster sizes, and if so, do they all have similar shapes*? Our results (Sec. IV A) indicate that Ag_{10} has only one abundant isomer, whereas Ag_n ($n=8,9,11,12$) most likely exhibit two or more isomers. However, the low energy isomers that possibly coexist share structural similarities (Sec. V). It is possible that the properties of these isomers are indistinguishable, and that they appear as if they were a single chemical species. *Is it important to know details of the structure of silver clusters*? We show (Sec. V) that many important aspects of structure can be expressed with a number of descriptors that is much smaller than the number of degrees of freedom. However,

a)Electronic mail: renef@yorku.ca

one can not ignore nuclear positions entirely, as in the spherical jellium model, or characterize clusters adequately using only, for instance, the three moments of inertia. Furthermore, one needs the optimized geometries of the lowest energy isomer(s) in order to get quantitative accuracy on some properties, such as the ionization potential (Sec. IV C).

Describing clusters that may be nonrigid by means of a *structure* is not straightforward. One can think in terms of descriptors (e.g., moments of inertia) that are dynamically averaged for an individual cluster, or averaged with Boltzmann weight factors over a collection of rigid isomers. The main results reported here were obtained from standard clamped nuclei electronic structure calculations, so we favor the latter point of view. But other descriptions may be more appropriate. For example, one could sample configurations from a constant temperature simulation, map these configurations to the corresponding local minima by steepest descent, characterize the structure of the minima, and give the number of times each minimum is visited during a simulation.[43]

Here we will look at general aspects of structure and make only tentative predictions about specific silver clusters. We are mainly concerned with the energy distribution of isomers, their shapes, their vibrational frequencies, and principles that govern the energetically favored structures. Our main results come from Kohn–Sham (KS) density functional theory (DFT) calculations. We also used simple models in trying to explain different aspects of the *first-principles* results.

The rest of the paper is organized as follows: the next section gives details of the calculations. In Sec. III, we review the literature relevant for us with comparisons to our KS-DFT calculations. The main results of the calculations are in Sec. IV (relative isomer energies, atomization energies, electronic structure, and harmonic frequencies). Section V describes cluster geometry by means of descriptors and tries to account for the KS-DFT structures with simple ideas and models. A summary and conclusions are in Sec. VI.

II. COMPUTATIONAL DETAILS

We did KS-DFT calculations with the program deMon-KS3p2[44] using the basis sets and scalar relativistic model core potential developed by Andzelm *et al.*[45] The innermost orbitals are described by a model potential and projectors that enforce orthogonality between core and valence, and 17 electrons per silver atom (nominally $4p^6 4d^{10} 5s^1$) are treated explicitly. The grid for numerical evaluation of exchange-correlation terms had 64 radial shells of points, and each shell had 50, 110, or 194 angular points depending on the distance to the nucleus (''FINE'' option in deMon). Gradients of the energy were calculated analytically, except for the usual numerical handling of exchange-correlation. Trial geometries were optimized by a standard quasi-Newton method until the norm of the gradient was typically 5×10^{-5} atomic units (a.u.) or less for the lowest energy isomers; for isomers that were clearly high in energy, we stopped optimization when the norm of gradient was about 5×10^{-4} a.u. or even earlier. Even in those cases, the energy is almost certainly within 0.05 eV of the local minimum.

We decided to use the local spin density (LSD) approximation implemented via the Vosko–Wilk–Nusair exchange-correlation functional[46] instead of one of the more recent functionals. The VWN functional has a modest but well-documented accuracy. Newer functionals are in closer agreement with experiment for geometries and binding energies in organic molecules, but they do not give systematic improvements for solids, and very little is known about their performance for metallic systems. The meta-GGA functionals are promising,[47] but there are many different versions of them, they are not all readily available, and they have not been tested sufficiently for a meaningful study of trends in metal clusters. Semi-empirical functionals used in quantum chemistry are not a good choice for metal clusters because they are parametrized by fitting to databases where there are no metal–metal bonds. They are also unsatisfactory for theoretical reasons explained in Ref. 47. In particular, the B3LYP hybrid functional gives disappointing results for transition metal dimers.[48,49] It does not seem significantly better or worse than LSD for metals. The B3LYP functional includes some Hartree–Fock exchange, and Hartree–Fock theory always gives a zero density of states at the Fermi level. The use of Hartree–Fock or B3LYP is problematic for metal clusters whose properties should converge to the bulk metal with increasing size.

We did calculations on Ag_2 with two local and four gradient-corrected functionals and found that, compared to experiment, VWN gives the best bond length (2.504 Å versus 2.530 96),[50] a harmonic frequency of 206 cm^{-1} (expt. 192 cm^{-1}),[51] which is nearly as good as the best gradient-corrected functional, and a dissociation energy of 2.22 eV (expt. 1.66),[51] which overestimates the true value. Local spin density calculations almost always overestimate binding energies (by up to 100%) and harmonic frequencies (typically by 10% to 20%), they under estimate bond lengths (typically by 1% to 2%), and give good energy differences between systems with equal number of bonds. We found that, for silicon, a simple shift of the atom's energy brings VWN cluster atomization energies[52] in excellent agreement with experiment and high-level calculations.[53] Accordingly, we shifted the silver atom's energy down by $(2.22-1.66)/2 = 0.28$ eV before calculating the atomization energies of Table I.

Gradient-corrected functionals are more sophisticated and more costly in computer time, but they appear to be less reliable than LSD for silver cluster structures and energies. We report gradient-corrected results for some of the most important silver cluster isomers in Sec. VI, and contrast them with LSD results. Except for Sec. VI, we discuss only LSD results.

We did a thorough search for the lowest energy structures, but we cannot claim to have found the global minima. For Ag_n clusters with $n<9$, we did calculations on structures already reported in the literature[39] and a few additional ones. Our strategy in searching for the global minima of Ag_n for $n \geqslant 9$ was to take as candidate structures all those derived by capping the most stable $Ag_{(n-1)}$ isomer, the ten (or so) lowest n-atom cluster isomers obtained with a Lennard-Jones (LJ) potential, and a few more structures with high-

TABLE I. Atomization energy (eV) and structural descriptors (see Sec. V) for the most stable silver cluster isomers. See Sec. IV A for the notation and abbreviations used.

	Cluster	A (eV)	ρ	γ	δ	ζ	η
2.1		1.662					
3.1	C_{2v} isosceles tri	2.582	2.67	2.00	0.00	0.36	−0.25
4.1	D_{2h} rhombus	4.875	2.63	2.50	0.25	0.57	0.31
5.1	C_{2v} trapezoid	6.806	2.62	2.80	0.56	0.51	0.18
6.1	D_{3h} triangle	9.477	2.61	3.00	1.00	0.33	−0.49
7.1	D_{5h} PBP	11.547	2.70	4.57	0.82	0.13	−0.34
7.2	C_{3v} TCT	11.379	2.67	4.29	1.35	0.10	−0.30
8.1	D_{2d} DD	14.243	2.67	4.50	0.25	0.06	0.28
8.2	T_d TT	14.228	2.67	4.50	2.25	0.00	0.00
9.1	C_s B-DD	15.895	2.68	4.67	0.67	0.19	0.42
9.2	C_{2v} 12-PBP	15.875	2.68	5.11	1.65	0.10	−0.08
9.3	C_{2v} 11′-PBP	15.845	2.69	4.89	2.32	0.07	0.28
9.4	C_1 A-DD	15.842	2.67	4.67	0.89	0.07	−0.02
10.1	D_{2d} twinned PBP	18.501	2.69	5.20	2.16	0.19	0.46
11.1	C_1 123′4′-PBP	20.610	2.69	5.46	2.07	0.25	0.22
11.2	C_1 11e23-PBP	20.463	2.67	5.46	2.43	0.18	0.06
12.1	C_s 1234′5′-PBP	23.263	2.68	5.67	2.39	0.21	0.08
12.2	C_1 irregular	23.188	2.67	5.33	1.56	0.21	0.10
12.3	C_1 multic-PBP	23.108	2.67	5.33	1.39	0.18	0.09

symmetry (e.g., bicapped square antiprism at $n=10$) or obtained by removing atoms from a 13-atom O_h cuboctahedron fragment of fcc crystal. For each of these structures we guessed the optimal Ag–Ag bond lengths from previous calculations, took a few (typically 7) steps with a standard quasi-Newton local optimization algorithm, ranked isomers by increasing energy, and then carried on full optimization of clusters that were roughly within 1.0 eV of the best one (typically about ten structures). We looked at Ag_{11} last and optimized fewer structures because comparisons with energies of 10- and 12-atom cluster isomers, along with short partial local optimization (3 steps), allowed us to quickly rule out many structures.

We did normal mode analyses by finite difference of gradients only for the most stable clusters of each size. This is required to find whether a stationary point on the potential surface is a minimum. But normal mode analysis is not overly important here for two reasons. First, the harmonic frequencies of all but the smallest silver clusters tend to be very similar from one isomer to another. The low frequencies are the most interesting because they could help identify nonrigid clusters; but low frequencies are notoriously difficult to calculate accurately, and here they should be taken only in a semiquantitative sense. Second, there is an important difference between metal clusters and covalently bonded molecules. In molecules, saddle points on the energy surface often correspond to breaking localized chemical bonds; they are very different from molecules near equilibrium. This is not normally the case in metals. There is a smooth change in the electronic structure of a metal in going from a minimum to a saddle point. Since we are interested in general aspects of the structure of clusters that could be nonrigid, saddle points are almost as relevant as minima.

III. REVIEW OF THE LITERATURE

There have been very many articles published on silver clusters and we will only review those most relevant to this work. The spectroscopic parameters that we calculate by VWN, and the experimental ones (in parentheses), for the diatomic molecule are: a bond length of 2.50 Å (2.530 96),[50] a dissociation energy of 2.22 eV (1.623),[54] and a harmonic frequency of 206 cm^{-1} (192).[51] These deviations from experiment for Ag_2 are typical of the VWN method.

The *trimer* has been studied extensively by different techniques.[31–33,55–62] Experiments give strong evidence that Ag_3 is a Jahn–Teller distorted isosceles triangle,[32,33,55,56] likely an obtuse triangle, but we are not aware of any experimental bond length or angle determination. Calculations give values that range from 63° to 84° for the large angle, with the best values close to 68°, and from 2.58 to 2.76 Å for the short bond lengths with the best value probably being close to 2.68 Å (see Ref. 31 and references therein). Our VWN calculation gives 69° and 2.56 Å. It underestimates the bond length, but apparently gives a good value for the angle. Analysis of experimental spectra is greatly complicated by the dynamic Jahn–Teller effect for the ground state, and maybe some excited states, and the presence of isotopomers. There are several conflicting determinations of the fundamental frequencies of the symmetric stretch (ω_s) and doubly degenerate asymetric stretch (ω_e) modes: $\omega_s=161\ cm^{-1}$ and $\omega_e=96\ cm^{-1}$;[55] $\omega_s=180\ cm^{-1}$ and $\omega_e=67\ cm^{-1}$;[56] $\omega_s=121\ cm^{-1}$ and $\omega_e=99\ cm^{-1}$;[33] $\omega_s=158\ cm^{-1}$ and $\omega_e=140\ cm^{-1}$;[32] and $\omega_s=129\ cm^{-1}$ (average of four isotopomers).[59] Resonance Raman spectra in cold matrix showed bands at 120.5 cm^{-1} in Kr[63] and 111 cm^{-1} in Kr and Xe[64] which were assigned to Ag_3. On the whole, experiments put ω_s around 150 cm^{-1} and ω_e around 100 cm^{-1}, with both of them being very uncertain. We simply calculated VWN harmonic frequencies for a permanently distorted C_{2v} triangle and got 209, 142, and 66 cm^{-1}. The smaller frequencies and their average, 104 cm^{-1}, are not inconsistent with the degenerate ω_e of fluxional Ag_3 found in most experiments. The highest VWN frequency is surely higher than the true ω_s. This is probably due to VWN bond lengths

being too short, but also maybe partly to the harmonic approximation and static C_{2v} structure that we used, instead of the true dynamic symmetry (D_{3h}). In any case, it is unlikely that the higher VWN frequency would be in error by more than 50%, so it gives support to the higher values of ω_s.

Dissociation energies have been measured by collision induced dissociation for Ag_n^+ up to $n=25$,[65] and for Ag_n^- up to $n=11$.[66] Dissociation energies of Ag_n^- ($n=7$ to 11) were also obtained by analyzing the kinetics of photodecomposition.[67] When combined with vertical ionization potentials (IP)[68,69] and electron affinities (EA),[70–74] they yield dissociation energies of neutral clusters, but these have large uncertainties. The IP's show evidence of electronic shells and strong even-odd oscillations, as do the dissociation energies. The size dependence of the IP's is highly structured and indicates that silver clusters can not be treated as simple jellium spheres, their geometries are nonspherical.[68,69] Photoelectron spectra of the anion clusters have been studied in much detail.[70–74]

The association complexes of Ag_n with NH_3,[12,75] CH_3OH,[16] C_2H_4, and C_2H_4O[15] have been characterized experimentally. These complexes were used as models for adsorption, diffusion, and reaction on silver surfaces. The binding of C_2H_4 and C_2H_4O to silver clusters is similar to that observed on silver surfaces.[15] Ammonia bonding to silver clusters shows size-dependent properties: The measured binding entropies indicate that NH_3 is mobile on many silver clusters, but locally bound on some.[12,75]

Optical absorption spectra have been reported for Ag_n embedded in solid argon[76,77] ($n=3$ to 40), and for gas-phase Ag_n[12,78] ($n=4,7,9,10,12$) and a few Ag_n^+ clusters.[79] The spectra of Ag_4 and Ag_7 are very simple, but those of Ag_{10}, Ag_{12}, and especially Ag_9, have many peaks which suggest low symmetry or multiple isomers. We did find many isomers for Ag_9 (Sec. IV A). Optical absorption[80] and Raman scattering[81] experiments were done for larger clusters embedded in a matrix. Haslett and co-workers reported the Raman spectra of silver clusters isolated in a matrix of solid argon and identified the structure of Ag_5[35] as the planar trapezoid (5.1 in Fig. 1) and that of Ag_7[36] as the tetracapped tetrahedron (7.2 in Fig. 1).

On the theoretical side, Bonačić-Koutecký and coworkers did a comprehensive study of structural isomers of Ag_n^+ and Ag_n,[39] and Ag_n^-[82] ($n=3$ to 9) by Hartree–Fock and correlated *ab initio* methods. According to their configuration interaction calculations, the isomers within 0.2 eV of the most stable for each size are (refer to Table IV for the notation, and Fig. 1): 4.1; 5.1 and 5.2; 6.2 and 6.3; 7.1; 8.1 and 8.2; and 9.2. This agrees with our VWN results on many points, but there are discrepancies as well: We find 5.2 to be unstable; for Ag_6 the lowest energy structure is different; and for Ag_9, we find many more isomers in addition to 9.2. Bonačić-Koutecký *et al.* also studied the absorption spectra of Ag_n^+ and Ag_n[34] ($n=2$ to 4), showing, in particular, strong evidence for the rhombus geometry of Ag_4, and calculated the electron impact ionization cross-sections of Ag_n ($n=2$ to 7).[83] References to several theoretical studies prior to 1998 can be found in the article by Bonačić-Koutecký and coworkers (see citations number 10 to 31 in Ref. 34). These studies dealt mostly with small clusters ($n<6$).

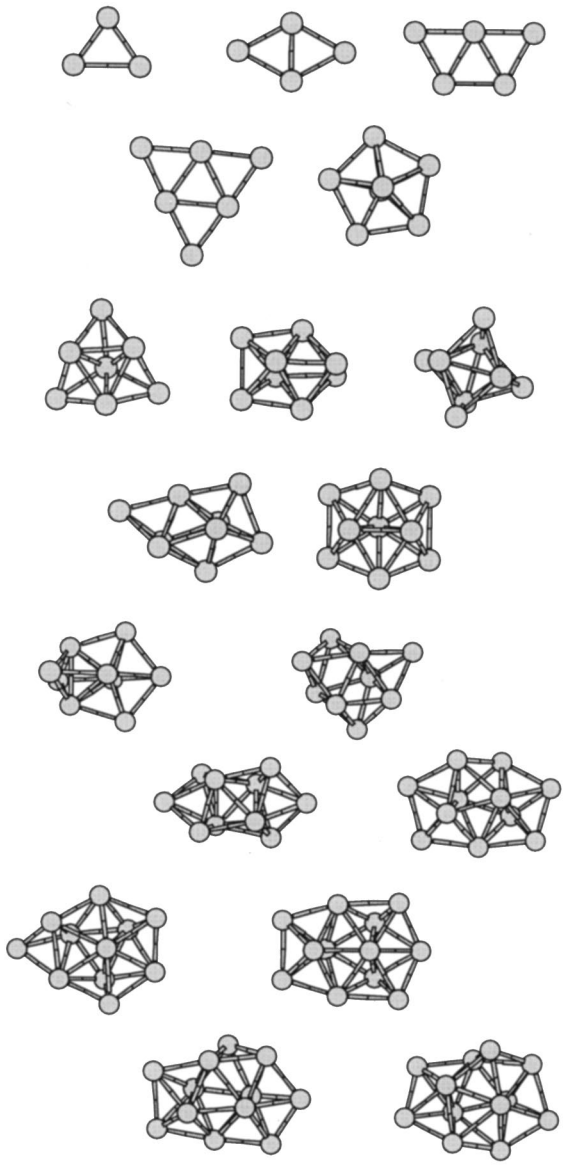

FIG. 1. The lowest energy Ag_n isomer of each size, and isomers within 0.18 eV of them, ordered (from left to right and top to bottom) by increasing size and energy.

IV. KOHN–SHAM LOCAL SPIN DENSITY RESULTS

A. Relative isomer energies

We optimized geometries and calculated energies for 68 isomers of Ag_n ($n=3-12$). We do not report all the optimized structures here, but their cartesian coordinates are available upon request to the author. Figure 1 shows the lowest energy isomer, and those within 0.18 eV of the lowest, for each size. We assign labels to clusters such as 7.1 or 9.3; the first number indicates the number of atoms and the second gives the rank in increasing energy order. Hence, 9.3 is the third most stable 9-atom cluster. Some structures have special importance because they are building blocks for larger clusters. They are: the 6-atom O_h octahedron (O); the D_{5h} pentagonal bipyramid (PBP) 7.1, and C_{3v} tricapped tetrahe-

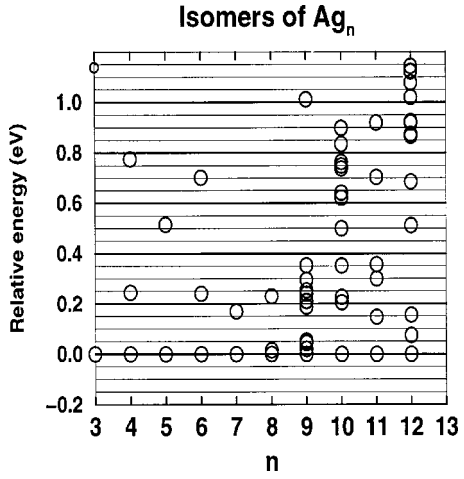

FIG. 2. Relative energy of Ag_n cluster isomers (eV).

dron (TCT) 7.2, both of which have been identified experimentally; the D_{2d} dodecahedron (DD) 8.1, which can also be viewed as a distorted bicapped octahedron; the T_d tetracapped tetrahedron (TT) 8.2; the D_{2d} twinned PBP 10.1; and, the ideal 13-atom I_h icosahedron and O_h cuboctahedron from which smaller clusters can be obtained by removing atoms. Many of the larger stable clusters can be obtained by successive cappings of triangular faces or edges of the octahedron (O), PBP, DD, or TT. We denote any of the symmetry equivalent triangular faces of an octahedron or PBP by 1, and we number the other triangular faces in sequence according to their position relative to the first one: On the same side of the equatorial plane are 2 and 3, while $1'$, $2'$, etc., are on the other side of the equatorial plane. For example, we denote the five distinct bicapped PBP by 12-PBP, 13-PBP, $11'$-PBP, $12'$-PBP and $13'$-PBP, and the three distinct bicapped octahedra 12-O=$11'$-O, 13-O=$12'$-O, and $13'$-O. We represent capping of the edge common to 1 and $1'$ by the symbol ''1e.'' Thus, the D_{2d} twinned PBP 10.1 can be described as a $11'$-PBP with a tenth atom capping the $11'$ edge of the PBP or, for short, $11'$1e-PBP. The DD has two distinct triangular faces: four at the ends which we denote ''A'' and eight on the sides which we denote ''B.'' Here are some other abbreviations that we use in the tables: for trigonal bipyramid, ''TBP''; for square antiprism, ''SAP''; to denote a cluster formed by deleting n atoms from a O_h cuboctahedron, ''cubo-n'' likewise, ''ico-n'' for deleting from the icosahedron; ''bic,'' ''tric,'' ''tetrac,'' and ''multic'' for bicapped, tricapped, tetracapped, and multicapped, respectively; to denote capping at a triangular face formed by a previous capping.

Figure 2 shows the calculated isomer energies relative to the most stable of each size. Many isomers that we considered are not shown on this diagram because their energies are too high. We expect these relative energies to be accurate to within roughly 0.2 eV. Taking this as a guideline, our calculations support the previous structure assignments for Ag_3 (slightly obtuse C_{2v} triangle), Ag_4 (rhombus), and Ag_5 (trapezoid), and predict that Ag_6 is a planar D_{3h} triangle and Ag_{10} is a D_{2d} twinned PBP. The structure of Ag_7 is problematic. The calculations indicate that the D_{5h} PBP is favored by 0.17 eV over the C_{3v} TCT, in agreement with electron spin resonance experiments.[37] But a comparison of the observed Raman spectrum to simulated spectra based on DFT calculations clearly favors the C_{3v} TCT.[36] We favor the latter because the simulated Raman spectrum is very sensitive to structure. However, considering the small calculated energy difference between D_{5h} PBP and C_{3v} TCT, it is possible that experimental details can favor the formation of one or the other isomer. The energy difference between 8.1 and 8.2 is very small and does not allow prediction of structure. There are four isomers of Ag_9 within 0.05 eV of each other obtained by different capping of the PBP and DD. While we cannot predict the structure of Ag_9, these energies are a strong indication that many isomers of Ag_9 are probably observed in experiments. For Ag_{11} and Ag_{12}, the relative energies suggest that, unlike Ag_9, only one or two structures would be seen in low-temperature experiments.

To sum up, the low-energy structures of Ag_n evolve from planar for $n=3$ to 6, to high-symmetry and compact for $n=7$ and 8, to a coexistence of many bi-capped PBP and capped DD at $n=9$, and finally to prolate structures obtained by successive cappings of the PBP for $n=10$, 11, and 12. We give a more detailed analysis in Sec. V.

B. Size dependence of energies

There are different ways to present the size dependence of cluster energies. In Table I and Fig. 3 we report: (a) atomization energies ''A'' corresponding to $Ag_n \rightarrow n\,Ag - A$ eV; (b) binding energies ''BE'' corresponding to $Ag_n \rightarrow Ag_{n-1} + Ag - BE$ eV; (c) cohesive energies, A/n; and (d) disproportionation energies ''D'' for $2\,Ag_n \rightarrow Ag_{n-1} + Ag_{n+1} - D$ eV. The VWN energy of the single silver atom was shifted so as to reproduce the known dissociation energy of the diatomic, 1.66 eV. All other energies were taken directly from VWN calculations. We calculated vibrational frequencies for some of the clusters, but the energies that we report here *do not include* the zero point energy (ZPE). The ZPE is small for silver clusters and it has a nearly constant value of 0.007 eV (60 cm^{-1}) per degree of freedom.

With the empirical correction to the silver atom energy, we expect that our VWN binding and cohesive energies would both converge to a value close to 2.95 eV, the experimental bulk cohesive energy E_c (bulk), at large cluster size. The largest binding energy (2.70 eV, for Ag_8) and the binding energy of Ag_{12} (2.65 eV) are within 10% of E_c (bulk); but the largest cohesive energy (1.94 eV, Ag_{12}) is only two-thirds of E_c (bulk) and the cohesive energy increases only slowly with size. There is an even-odd oscillation in cluster energies which is most obvious when we look at disproportionation [Fig. 3(b)]. The mean absolute value of the disproportionation energy is 0.75 eV. If we look separately at even and odd numbered clusters, for example reactions of the type $2\,Ag_n = Ag_{n-2} + Ag_{n+2}$, we still see appreciable variations (on the order of ± 0.5 eV) in relative stabilities. If we leave aside the obvious even-odd oscillations and overall increase in binding energies with size, the 7- and 8-atom clusters appear more stable than the rest, whereas Ag_9 appears the

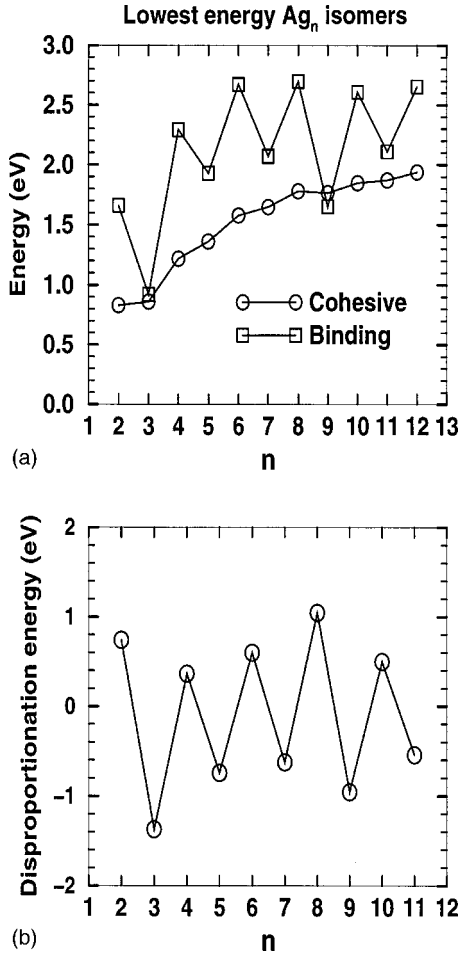

FIG. 3. Energies (eV) of the most stable cluster isomers of each size: (a) cohesive and binding energies, and (b) disproportionation energies.

least stable. The PBP 7.1 and DD 8.1 are also important structural motifs in the larger clusters.

By combining the experimental EA[70] and collision induced dissociation energies of the anions,[66] one can get experimental atom binding energies for the neutral clusters. Unfortunately, the uncertainty on these is large, on the order of 0.2 to 0.5 eV. Bearing this in mind, our calculations and experiments agree on many points: Ag_8 has the largest BE and it is close to 2.7 eV; Ag_9 has the smallest BE and it is close to 1.5 eV; other BEs in the range $4 \leqslant n \leqslant 11$ are between 1.9 and 2.6 eV. There is disagreement about the BE of Ag_6 which we calculate to be 2.67 eV, but is much smaller according to experiment (apparently around 2.0 eV).

C. Electronic structure

The energies of the highest occupied molecular orbital (HOMO) and lowest unoccupied molecular orbital (LUMO) correlate very well with the relative isomer energies and IP's of the clusters. The HOMO–LUMO gap varies between 0.15 and 0.27 eV among odd-numbered clusters: 7.1 has the largest value (0.27 eV) and is the most stable in that group. The gaps for the isomers N.1 (see Table II) are the largest for every even N with two exceptions: the linear 4.3 (1.2 eV) and tetrahedral 8.2 (2.5 eV). The latter has essentially the same energy as 8.1. The HOMO–LUMO gaps of the various even-N isomers span the range between zero and these maximal values. A few isomers of Ag_{10} and Ag_{12} have triplet ground states: the most stable among them have energies of +0.90 eV and +0.69 eV relative to 10.1 and 12.1, respectively.

TABLE II. HOMO–LUMO energy gap, and vertical ionization potential (eV) of the most stable cluster isomers.

			Vertical IP		
	Cluster	Gap	Calc.	Expt.[a]	Diff.
2.1		2.3	8.58	7.60	0.98
3.1	C_{2v} isosceles tri	0.2	6.34	6.20	0.14
4.1	D_{2h} rhombus	0.9	7.16	6.65	0.51
5.1	C_{2v} trapezoid	0.3	6.74	6.35	0.39
6.1	D_{3h} triangle	2.4	7.69	7.15	0.54
6.2	C_1 1e-TBP	0.7	7.48	”	0.33
6.3	C_{5v} pyramid	1.9	7.48	”	0.33
7.1	D_{5h} PBP	0.3	6.50	6.40	0.10
7.2	C_{3v} TCT	0.2	6.60	”	0.20
8.1	D_{2d} DD	1.8	7.24	7.10	0.14
8.2	T_d TT	2.5	(7.50)	”	0.40
8.3	C_s 1-PBP	1.4	6.84	”	−0.26
9.1	C_s B-DD	0.2	6.45	6.00	0.45
9.2	C_{2v} 12-PBP	0.2	5.88	”	−0.12
9.3	C_{2v} 11′-PBP	0.2	5.73	”	−0.27
9.4	C_1 A-DD	0.2	(5.77)	”	−0.23
10.1	D_{2d} twinned PBP	1.0	6.45	6.25	0.20
10.2	C_1 11e2-PBP	0.8	(6.36)	”	0.11
10.3	C_s 124′-PBP	0.8	(6.60)	”	0.35
10.4	C_1 11′3-PBP	0.8	(5.96)	”	−0.29
11.1	C_1 123′4′-PBP	0.2	6.34	6.30	0.04
11.2	C_1 11e23-PBP	0.2	6.04	”	−0.26
12.1	C_s 1234′5′-PBP	0.9	6.66	6.50	0.16
12.2	C_1 irregular	0.9	6.53	”	0.03
12.3	C_1 multic-PBP	0.7	6.35	”	−0.15

[a]Reference 69.

Calculated vertical IP's are given in Table II. The difference between vertical IP and HOMO energy is usually within ±0.02 eV (and always within ±0.07 eV) of the mean for a given cluster size. The (IP–HOMO) for clusters with 2 to 12 atoms are 2.90, 2.34, 2.25, 2.13, 2.08, 2.03, 1.97, 1.81, 1.82, 1.74, and 1.73 eV. The IP's shown in parentheses in Table II are empirical estimates based on the HOMO energy and the mean of (IP–HOMO) for clusters of the same nuclearity. In cases where the structure is known (2.1, 3.1, 4.1, and 5.1), the calculated vertical IP's overestimate experimental values[69] by 0.98, 0.14, 0.51, and 0.39 eV, respectively, while the average of 7.1 and 7.2 overestimates by 0.15 eV. From this, we expect that the calculated IP's for Ag_n ($6 \leqslant n \leqslant 12$) to be within −0.2 eV and +0.4 eV of experiment, provided that the structures are correct. Using this as a guideline, the comparison of IP's does not allow us to say anything about the structure of Ag_7, Ag_9, and Ag_{12}, but it almost rules out 8.3, 10.4, and 11.2 as possible observed structures. The structure we would predict for Ag_6 on the basis of VWN energies, 6.1, is in doubt; its IP does not agree with experiment, and other calculations do not show 6.1 as particularly stable.[39] We think that VWN is biased toward planar structures and that the true most stable isomer of Ag_6 is *not* 6.1. Many isomers of Ag_9 with nearly equal VWN energies are likely to coexist in experiments. None of them has an IP equal to the

experimental value of 6.00 eV. They are either too high and close to 6.45 eV (9.1, 9.6, and 9.8), or too low and close to 5.80 eV (9.2, 9.3, 9.4, 9.5, 9.7, 9.9, and 9.10). The unusually large drop in IP from Ag_8 to Ag_9 observed by Jackschath *et al.*[69] and Alameddin *et al.*[68] could be due to an averaging effect that includes several isomers of Ag_9 with low IP that are only slightly higher in energy than 9.1.

Bérces *et al.* used an effective IP, defined as the cluster IP plus a polarization energy, to discuss the anticorrelation of IP and reactivity in niobium clusters.[19] Following them, we write the IP of a hypothetical metal sphere, IP°, as

$$\mathrm{IP}^\circ = \mathrm{WF} + \frac{e^2}{2(R_c + a)}, \tag{1}$$

where WF is the bulk metal work function (4.64 eV for silver), R_c is the radius of the spherical cluster, and a is the extent of electron density spillout. In order to calculate R_c, we assume that atoms pack as closely in a cluster as in a fcc crystal so that we can assign them atomic volumes equal to $(R_a^3\sqrt{2}/2)$, where R_a is half a typical distance between nearest neighbors in the cluster. We take $R_a = 2.7$ Å by average over our VWN optimized geometries. We initially took $a = (R_a/2) = 1.35$ Å, but after test calculations we modified it to $a = 1.215$ Å. The radius of the hypothetical spherical cluster is

$$R_c = R_a n^{1/3} 3\sqrt{2}(8\pi). \tag{2}$$

We calculated IP° by Eqs. (1) and (2). Of course IP° varies smoothly with size and does not agree very well with experiment. We are interested in the *differences* between IP° and the VWN cluster IP because these will show specific effects of size and structure on IP's. The difference (IP–IP°), in eV, for isomers N.1 (N=3 to 12) are: −0.44, 0.51, 0.19, 1.22, 0.09, 0.89, 0.14, 0.18, 0.11, and 0.47. With the exception of clusters 3.1 and 10.1, (IP–IP°) is close to half the HOMO–LUMO gap which is, itself, relevant to chemical reactivity. Removing the trivial IP° from actual cluster IP's gives another way to look at the relation between cluster IP and reactivity.[19]

D. Harmonic frequencies

We did a normal mode analysis for the following structures: all N.1 isomers, 7.2, 8.2, 9.2, and 9.4. In all cases, we found (3N−6) real frequencies, and it seems very likely that structures within a few tenths of an eV of N.1 are minima as well. The lowest, mean, and largest frequencies for each of the N.1 isomers are shown in Table III. There is a noticeable jump in the largest frequency from $N=6$ to $N=7$ clearly due to the change from planar to 3D structure. This could be useful in elucidating the structure of Ag_6 because the largest frequency is a breathing mode for which we expect intense Raman activity. We calculated the vibrational contribution to the enthalphy at 298 K.[84] It amounts to about 0.44 kcal/mol per degree of freedom for all clusters at which we looked. All clusters have some very low frequencies, lower than that of Ag_3. We take this as an indication that silver clusters could be nonrigid at room temperature. The calculated frequencies and relative isomer energies suggest that most silver clusters are neither liquidlike nor rigid at room temperature. They probably undergo large amplitude motions along certain modes, but for most cluster sizes, the isomer energy separations seem too large to allow frequent isomer interconversion. Clusters Ag_8, Ag_9 (and maybe also Ag_{12}) look different. They have relative isomer energies of the same order as room temperature and not much larger than typical harmonic frequencies, so frequent isomer interconversion and liquidlike behavior appear possible.[42]

TABLE III. Lowest, mean, and largest harmonic frequencies (cm^{-1}) for some of the most stable isomers.

Cluster		Frequencies		
3.1	C_{2v} tri	66	139	209
4.1	D_{2h} rhombus	45	128	216
5.1	C_{2v} trapezoid	29	119	224
6.1	D_{3h} triangle	31	117	231
7.1	D_{5h} PBP	36	115	194
7.2	C_{3v} TCT	25	117	194
8.1	D_{2d} DD	56	118	196
8.2	T_d TT	23	118	194
9.1	C_s B-DD	40	113	202
9.2	C_{2v} 11′-PBP	43	111	208
9.4	C_1 A-DD	46	114	195
10.1	D_{2d} twinned PBP	35	114	198
11.1	C_1 123′4′-PBP	44	113	199
12.1	C_s 1234′5′-PBP	37	112	204

V. STRUCTURE OF SILVER CLUSTERS

It is not practical to discuss the structure of N-atom clusters in terms of $(3N-6)$ (or $3N$) nuclear coordinates. By using, instead, m shape descriptors ($m \ll 3N-6$), we lose details, but we can gain insight and a convenient way of comparing clusters of different sizes. It is important to select descriptors that are appropriate for the systems and properties under study.[85] Here we use five descriptors which, we think, play an important role for the relative energies of silver clusters. We define the nearest-neighbor distance for a given atom "k" ρ_k as the average of the two shortest distances from atom k to other atoms in the cluster (or just the shortest distance for some atoms in 4.2 and 4.3), and we define the mean nearest-neighbor distance ρ as the average of the ρ_k's in a cluster. We define the coordination number of an atom, c_k, as the number of atoms located within a sphere of radius 1.15ρ centered around atom k. Using the c_k's in a N-atom cluster, we calculate the mean coordination, γ, and the root-mean-square fluctuation among coordinations, δ:

$$\gamma = \sum_{k=1}^{N} c_k / N, \tag{3}$$

$$\delta = \left[\sum_{k=1}^{N} (c_k - \gamma)^2 / N \right]^{1/2}. \tag{4}$$

We derive two descriptors from the three moments of inertia $I_a \geq I_b \geq I_c$. We use the following definition of asphericity, ζ:

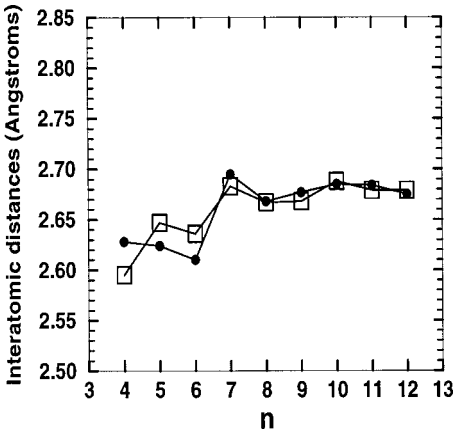

FIG. 4. Nearest-neighbor distance (ρ) averaged over all isomers for each size. Filled circles: Boltzmann weight factors with $\beta=10\,\mathrm{eV}^{-1}$. Open squares: Simple average (same weight for each isomer).

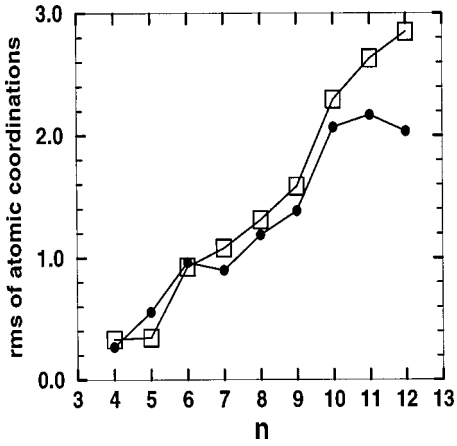

FIG. 6. Root-mean square deviation of atomic coordination around the average value (δ) averaged over all isomers for each size. Filled circles: Boltzmann average ($\beta=10\,\mathrm{eV}^{-1}$). Open squares: Simple average.

$$\zeta=\frac{(\mathrm{I}_c-\mathrm{I}_b)^2+(\mathrm{I}_b-\mathrm{I}_a)^2+(\mathrm{I}_a-\mathrm{I}_c)^2}{\mathrm{I}_a^2+\mathrm{I}_b^2+\mathrm{I}_c^2}. \tag{5}$$

Another descriptor, η, is used to distinguish between prolate and oblate clusters,

$$\eta=(2\mathrm{I}_b-\mathrm{I}_a-\mathrm{I}_c)/\mathrm{I}_a\,. \tag{6}$$

Together, the five descriptors ρ, γ, δ, ζ, and η, summarize important aspects of cluster structure: $N\rho^{1/3}$ scales with the *size* of the cluster and ρ approaches the bulk nearest-neighbor distance R_{NN} at large N; γ and δ depend on the *connectivity* between atoms; ζ and η describe the *shape*, they are both zero for a spherical cluster and the sign and magnitude of η tells how much a cluster is prolate (when $\eta>0$) or oblate (when $\eta<0$). The values of the descriptors for the most stable clusters are listed in Table I.

In order to allow easier comparisons, we performed *averages* of descriptors for each cluster size. We do these averages in either of two ways: (a) by assigning equal weights to each isomers; or (b) by assigning unequal Boltzmann weights $\exp(-\beta(\mathrm{E}_j-\mathrm{E}_0))$ to each cluster j, where E_j and E_0 are the atomization energies of isomer j and of the most stable isomer (''0'') of the same size. We chose $\beta=10\,\mathrm{eV}^{-1}$, not so much to simulate a temperature, but more to smooth out errors that come with VWN energies.

Average (a) depends on the structures (after local optimization) that were considered in the search for the global minimum. To see what characteristics are energetically favorable for silver clusters, one should look mainly at the averages (b), implicitly assuming that we did a good search for the global minimum. To a lesser degree, the *difference* between averages (b) and (a) also matters, because a poor choice of trial structures could cause an artificial bias in averages (b). Figures 4–8 show the two types of averages for each of the five descriptors.

The nearest-neighbor distance ρ (Fig. 4) is clearly shorter in the planar clusters $n=4$ to 6 where coordination is smallest (Fig. 5). There is a jump in ρ (and clearly also in γ) from $n=6$ to $n=7$. Surprisingly, ρ changes very little from $n=7$ to $n=12$ and it remains much smaller than the experimental bulk value of 2.89 Å. The VWN calculation underestimates the bond length of Ag_2 by 0.03 Å. Even if VWN underestimated the interatomic distances by 0.10 Å, the true

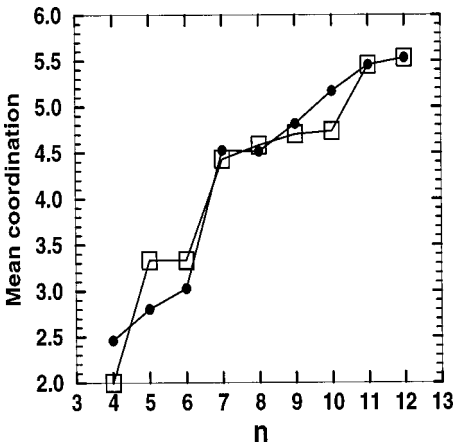

FIG. 5. Mean coordination (γ) averaged over all isomers for each size. Filled circles: Boltzmann average ($\beta=10\,\mathrm{eV}^{-1}$). Open squares: Simple average.

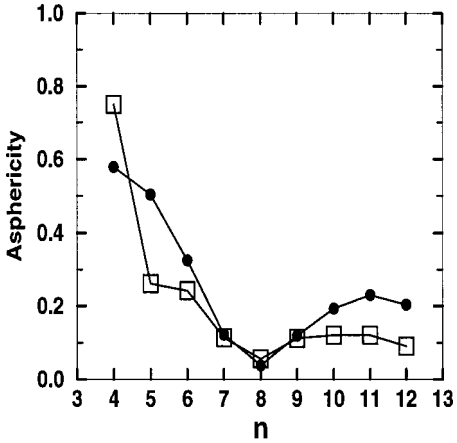

FIG. 7. Asphericity (ζ) averaged over all isomers for each size. Filled circles: Boltzmann average ($\beta=10\,\mathrm{eV}^{-1}$). Open squares: Simple average.

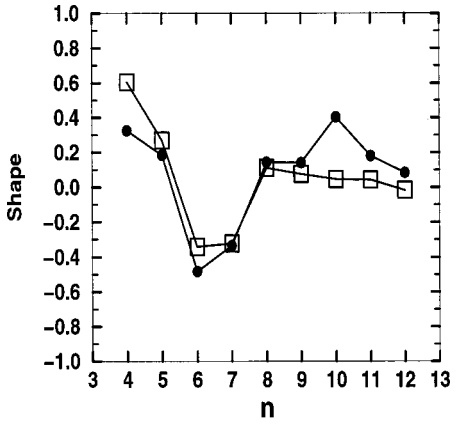

FIG. 8. Shape (η) averaged over all isomers for each size. Filled circles: Boltzmann average ($\beta = 10\,\mathrm{eV}^{-1}$). Open squares: Simple average.

ρ in 7- to 12-atom Ag clusters would still be about 0.10 Å less than the bulk nearest-neighbor distance.

The LJ potential favors structures with maximum coordination, and we expected the same for clusters of a simple metal like silver for $n \geqslant 7$. This is only partly true. The most stable LJ clusters are generally *not* very good structures for Ag_n. Their relative energies (eV) with respect to the best isomer for $n=7$ to 12 are as follows: 0.00, 0.23, 0.04, 0.64, 0.70, and 1.12, respectively. The Ag_n clusters do *not* maximize γ. However, γ tends to be close to maximum. It should be noted that the isomers considered in the search are not random, they are very compact, and that among these, the γ of the lowest energy structures are neither low nor high (compare filled circles and open squares in Fig. 5).

For $n \geqslant 7$, there is a clear preference for structures that minimize δ (Fig. 6). Although some clusters have small δ for reasons of symmetry (e.g., 7.1 and 8.1), there is in general no more correlation between high symmetry and small δ than there is between high symmetry and low energy. Clusters 9.1, 11.1, and 12.1 all have low symmetry, yet small δ. Conversely, many high-symmetry structures which we considered have a large δ (and a high energy). We suggest that, other things being equal, minimizing δ could be a useful heuristic principle for atomic cluster structure.

The descriptor ζ has a clear minimum near $n=8$ (Fig. 7) in very good agreement with the EJM.[41] This could be somewhat coincidental because there are not too many ways of making compact arrangements of a few hard spheres, and structures that maximize γ and minimize δ happen to have a small or zero value of ζ for $n=6$ to 9 for geometrical reasons. This is partly why the two kinds of averages are very close at $n=7$, 8, and 9 (Fig. 7). Note, however, that low-energy structures of Ag_{10}, Ag_{11}, and Ag_{12} are on average, more aspherical than the isomers for which we did calculations.

The descriptor η allows a more detailed comparison of the favored shapes. First, we look at the energetically favored structures (filled circles in Fig. 8). We left out Ag_3 because such a small cluster has too few possible isomers for average descriptors like η, or a model like the jellium, to be meaningful, and because the isosceles triangular structure of Ag_3 is well understood from high-level theory. This leaves nine cluster sizes for judging the validity of the simple EJM against KS-DFT. According to KS calculations, the 6- and 7-atom clusters are oblate ($\eta<0$), Ag_4 and Ag_{10} are "strongly prolate" ($\eta>0.2$), and all other clusters are "weakly prolate." The shapes predicted by the EJM agree rather well with DFT (Fig. 8 and Ref. 41) with one exception: Ag_5 is strongly oblate in the jellium model but prolate according to DFT. But for very small clusters, there is no reason to expect accurate predictions from the EJM. Indeed, aside from Ag_5, the EJM can be said to "fail" for Ag_4 because the highly prolate linear structure is much less stable than the moderately prolate rhombus. There are also subtle, but significant, differences between VWN and EJM among larger clusters. According to the EJM, 8.2 is favored over 8.1 by the shape ($\eta=0.00$ versus $\eta=0.28$ for 8.1). Despite this, and the fact that 8.1 and 8.2 have the same ρ and γ, the two isomers are equally stable. We think that the reason for this is that 8.1 has a much smaller δ (0.25 compared to 2.25). Also, contrary to EJM predictions, the VWN-stable Ag_{10} is a lot more prolate ($\eta=0.46$) than Ag_{11} and Ag_{12}. We think that this is because 10.1 has the largest γ among the prolate isomers of Ag_{10}. One isomer has a larger γ than 10.1 but it is oblate ($\eta=-0.28$). Two other isomers have a γ equal to that of 10.1: one is oblate and unstable (0.90 eV), the other is weakly prolate ($\eta=0.10$) and, as one would expect from EJM, it is the second most stable isomer, 10.2 (11e2-PBP). It is not always possible for all descriptors to assume their optimal values simultaneously, because of geometric constraints, and this causes discrepancies between predictions from the EJM and actual optimal cluster structures.

To summarize, the structural attributes of low-energy silver clusters appear to be, in decreasing order of importance: a high mean coordination (γ); a shape (η) that conforms to the EJM; and uniformity in atomic coordinations (small δ), whether or not this is accompanied by high symmetry. In general, these isomers also have relatively large HOMO–LUMO gaps, but this is related to having an optimal shape in the EJM.

The EJM is not very useful for structure prediction because it says nothing about the position of the atoms. In order to better understand factors that relate structure and energy, we did fixed geometry calculations on all the VWN-optimized isomers with two very simple theoretical models: Extended Hückel molecular orbital theory and an empirical model for the energy based on the atomic coordinations c_k of Eq. (3).

The extended Hückel molecular orbital (eHMO) theory is well known.[86] We used a simplified version of it with a single *s* atomic orbital, one electron per silver atom, and an empirical calculation of overlap instead of using actual atomic orbitals. We set the diagonal elements of the Hamiltonian matrix H_{ii} equal to the VWN 5s atomic orbital energy (-4.718 eV) and we take the overlap integrals to be $S_{ij} = \exp(-\alpha R_{ij})$. We chose $\alpha = 0.27\,\text{Å}^{-1}$ so as to give an overlap of 0.25 for a typical nearest-neighbor distance (2.70 Å). We use the Wolfsberg–Helmholtz formula $H_{ij} = 0.875 \times S_{ij} \times (H_{ii} + H_{jj})$ for the off-diagonal Hamiltonian matrix elements. With these choices the HOMO–LUMO gaps are reasonable, typically within 0.2 eV of the VWN values (the

latter vary between 0.25 and 2.50 eV among even-numbered clusters). We did not try to optimize the parameters in any way because eHMO structural predictions are not sensitive to the precise values of the parameters, and eHMO theory cannot give reliable quantitative predictions of cluster energies. We take the eHMO energy as the sum, over occupied spin-orbitals, of orbital energies.

The empirical potential that we use is motivated by the observation that, in many metallic systems, cohesive energies scale as the square root of the atomic coordination.[87] We take coordinations c_k as already defined and calculate the cluster binding energy as a sum of atomic contributions:

$$U = E_c \sum_k (c_k/12)^{1/2}, \tag{7}$$

where E_c is the bulk cohesive energy of silver (2.95 eV) and 12 is the coordination of a silver atom in a fcc crystal. We will refer to this model as SSAC for ''Sum of Square-roots of Atomic Coordinations.'' Notice that this simple formula is in error by only 3% when applied to diatomic silver (1.70 eV vs. the experimental 1.66 eV), and that it reproduces the exact cohesive energy in the bulk limit. The SSAC is a crude model, but it is accurate enough for our purpose, and it is probably preferable than more complicated models in trying to find structural principles. We used a more complicated version of the SSAC to calculate surface energies. These results will be reported elsewhere. The main problem with the SSAC and similar models (e.g., the embedded atom method) is that it ignores specific quantum effects caused by symmetry (electronic shells, Jahn–Teller distortion) and spin pairing (even-odd oscillation). Like the LJ potential, the SSAC predicts that the lowest energy structures are those that maximize γ — structures derived from successive capping of the D_{5h} PBP and I_h icosahedron. The additive LJ potential and SSAC differ mainly in the size dependence of atomization energies.

The jellium and SSAC models are, in a sense, opposite. In the EJM, the symmetry of delocalized quantum states of N electrons dictate where the nuclei go in an average sense. The SSAC potential does not explicitly treat electrons, and it predicts specific arrangements of atoms that tend to be as compact and symmetrical as possible. The jellium and eHMO models give similar predictions of cluster shape, although they come from very different physical approximations. The EJM and eHMO theory can be viewed as simple models that try to capture the most important quantum effects.

Table IV gives the relative energy of isomers as calculated by VWN, SSAC, eHMO and the average of SSAC and eHMO. In each case, energies are shifted so that the most stable isomer of each size is assigned a zero energy. The VWN results are certainly the most reliable and they agree with experiment in every known case (Ag_3, Ag_4, Ag_5, Ag_7). We believe that VWN generally gives good predictions of the lowest energy structures, so we rate the simple models according to their ability to reproduce VWN results.

It is clear from Table IV that SSAC and eHMO are both very poor at predicting relative isomers energies. Interestingly, the relative energies of the *average* of SSAC and

TABLE IV. Relative energies (eV) of isomers obtained by VWN, SSAC, eHMO, and the average of SSAC and eHMO (Avg). See Sec. IV A for the notation and abbreviations used.

Cluster		VWN	SSAC	eHMO	Avg
4.1		0.00	0.00	0.79	0.00
4.2	C_{2v} Y-shaped	0.24	0.62	0.30	0.07
4.3	linear	0.78	1.25	0.00	0.23
5.1	C_{2v} trapezoid	0.00	1.00	0.00	0.00
5.2	C_{2v} TBP	0.52	0.00	1.03	0.02
5.3	C_{2v} TBP	1.20	0.00	1.22	0.11
6.1	D_{3h} triangle	0.00	0.94	0.00	0.01
6.2	C_{5v} pyramid	0.24	0.39	0.54	0.00
6.3	C_1 1e-TBP	0.70	0.00	1.42	0.25
7.1	D_{5h} PBP	0.00	0.00	0.19	0.00
7.2	C_{3v} TCT	0.17	0.46	0.00	0.14
8.1	D_{2d} DD	0.00	0.30	0.17	0.10
8.2	T_d TT	0.02	0.49	0.00	0.11
8.3	C_s 1-PBP	0.23	0.00	0.27	0.00
9.1	C_s B-DD	0.00	0.71	0.30	0.25
9.2	C_{2v} 12-PBP	0.02	0.00	0.52	0.00
9.3	C_{2v} 11′-PBP	0.04	0.46	0.38	0.16
9.4	C_1 A-DD	0.05	0.73	0.30	0.26
9.5	C_s 132′-O	0.19	0.81	0.28	0.28
9.6	C_1 13′-PBP	0.19	0.43	0.36	0.13
9.7	C_1 1t1′-O	0.21	0.81	0.42	0.35
9.8	C_1 11e-PBP	0.21	0.40	0.49	0.18
9.9	C_s 13-PBP	0.24	0.44	0.44	0.18
9.10	C_1 1tt′-PBP	0.25	0.81	0.41	0.35
9.11	C_{2v} 11′1e-O	0.30	0.37	0.51	0.18
9.12	C_1 12′-PBP	0.35	0.44	0.58	0.25
9.13	C_{4v} SAP	1.01	3.58	0.00	1.53
10.1	D_{2d} twinned PBP	0.00	0.40	0.93	0.05
10.2	C_1 11e2-PBP	0.21	0.41	0.84	0.00
10.3	C_s 124′-PBP	0.23	0.71	0.85	0.16
10.4	C_1 11′3-PBP	0.35	0.86	0.54	0.08
10.5	D_{2h} AA′-DD	0.50	1.03	0.99	0.39
10.6	C_s 123-PBP	0.62	0.00	1.55	0.15
10.7	C_1 11′2-PBP	0.74	1.35	0.80	0.46
10.8	C_1 12-TT	0.75	0.90	0.81	0.23
10.9	C_1 BB′-DD	0.76	0.70	0.99	0.22
10.10	C_s cubo-3	0.84	1.63	0.64	0.52
10.11	C_s 11′2-PBP	0.90	0.44	1.30	0.25
10.12	C_1 cubo-3	1.50	2.46	0.63	0.92
10.13	C_s 12′3-PBP	1.65	0.86	1.30	0.46
10.14	C_s bic SAP	2.25	4.96	0.37	2.04
10.15	D_{4d} bic SAP	3.01	6.01	0.00	2.38
11.1	C_1 123′4′-PBP	0.00	0.36	0.06	0.01
11.2	C_1 11e23-PBP	0.15	0.40	0.00	0.00
11.3	C_s 122e3-PBP	0.30	0.43	0.05	0.04
11.4	C_1 11′1e2-PBP	0.36	0.41	0.24	0.13
11.5	C_s 1234-PBP	0.70	0.00	0.49	0.05
11.6	C_1 122′3-PBP	0.92	0.88	0.25	0.36
12.1	C_s 1234′5′-PBP	0.00	0.75	0.11	0.00
12.2	C_1 irregular	0.07	1.42	0.00	0.28
12.3	C_1 mc-PBP	0.16	1.40	0.15	0.35
12.4	C_2 122′2e3-PBP	0.51	0.80	0.50	0.22
12.5	C_2 anti bic-10.1	0.51	0.80	0.53	0.23
12.6	C_{2v} tetrac-TT	0.69	0.80	0.64	0.28
12.7	C_s 1234(23e)-PBP	0.87	0.80	0.51	0.22
12.8	C_1 12342e-PBP	0.88	0.81	0.56	0.25
12.9	C_s 11′-10.1	0.92	1.68	0.25	0.53
12.10	C_s irregular	1.02	1.99	0.04	0.58
12.11	C_1 12342′-PBP	1.08	0.82	0.75	0.36
12.12	C_s ico-1	1.12	1.23	0.86	0.62
12.13	C_{5v} ico-1	1.12	0.00	0.97	0.05
12.14	C_s 11′1e22′-PBP	1.14	0.83	0.74	0.35
12.15	D_{3h} 3-6-3	1.22	1.10	0.99	0.61
12.16	C_{2v} cubo-1	1.30	1.89	0.10	0.56

TABLE V. Spectroscopic parameters calculated for Ag_2 with the VWN, PVS, BP86, and BLAP functionals.

	D_e (eV)	R_e (Å)	ω_e (cm^{-1})
VWN	2.22	2.50	206
PVS	1.98	2.49	211
BP86	1.65	2.57	182
BLAP	1.30	2.66	150
Expt.[a]	1.66	2.530 96	192

[a]See Sec. II.

eHMO (rightmost column in Table IV), which we will call ''SSAC-eHMO,'' is in better agreement with VWN than either SSAC or eHMO. The root-mean-square deviations from VWN isomer energies (eV) are 0.81 for SSAC, 0.63 for eHMO, and 0.43 for SSAC-eHMO, whereas the root-mean-square average of the VWN energies themselves is 0.80 eV. Another comparison we can make is to rank isomers by increasing energy for the various models. Then we form sets of isomers that fall in the lower half, by energy, and count how many isomers are in common between the sets generated by VWN, SSAC, eHMO, and SSAC-eHMO. Comparing to VWN, SSAC gets 16.5 ''hits,'' eHMO gets 18, and SSAC-eHMO gets 21, out of a possible maximum of 29. Judging from this, SSAC-eHMO has some merits for predicting isomer energies, but SSAC and eHMO have no value. Focussing on the few lowest-energy isomers of each size makes SSAC-eHMO look even better compared to SSAC and eHMO. Of course these numbers would change somewhat if we implemented SSAC and eHMO differently; but SSAC-eHMO is clearly the better of the three models, and its relative energies do correlate with those of VWN. We conclude that the most stable isomers of Ag_n represent an optimum compromise between close packing of atoms, as predicted by SSAC (and embedded atom methods), and JT distortion due to orbital symmetry and electron count, which is the essence of structure prediction by eHMO (and the EJM). Although our SSAC and eHMO models are crude, it is doubtful that small changes in these models, or their parameters, would produce a useful method for structural predictions. The SSAC and eHMO models seem to capture different aspects of the physics controlling cluster structure. An empirical method that would combine the two in a nontrivial way (*unlike* a simple average) could be really useful for investigating the structure of metal clusters.

VI. GRADIENT-CORRECTED FUNCTIONALS

We repeated calculations for some of the lowest energy isomers using the gradient-corrected exchange functional of Becke,[88] combined with the gradient-corrected correlation functional of Perdew,[89] or with the kinetic-energy-density and Laplacian dependent correlation functional developed by Proynov *et al.*[90] We denote these two methods BP86, and BLAP, respectively. We also did some calculations with the gradientless exchange-correlation functional of Proynov *et al.*[91] denoted PVS. Table V shows our results for Ag_2,[92] and Table VI shows relative isomer energies obtained by LSD, PVS, BP86, and BLAP. We use the same labels in Table VI as in Table IV, hence, 7.1 is the pentagonal bipyramid for all functionals, even though it is the lowest energy structure only for LSD and PVS.

TABLE VI. Relative energies (eV) of isomers obtained with VWN, PVS, BP86, and BLAP functionals.

	VWN	PVS	BP86	BLAP
4.1	0.00	0.00	0.00	0.13
4.2	0.24	0.24	0.05	0.00
4.3	0.78	0.74	0.35	0.10
5.1	0.00	0.00	0.00	0.00
5.2	0.52	0.53	0.70	0.77
5.3	1.20	1.04	1.27	1.28
6.1	0.00	0.00	0.00	0.00
6.2	0.24	0.23	0.37	0.41
6.3	0.70	0.71	0.98	1.17
7.1	0.00	0.00	0.00	0.03
7.2	0.17	0.18	0.07	0.00
8.1	0.00	0.00	0.07	0.10
8.2	0.02	0.00	0.00	0.00
8.3	0.23	0.23	0.22	0.10

The PVS functional gives essentially the same structures and relative isomer energies as VWN (Table VI). It gives smaller binding energies than VWN, but after shifting the Ag atom energies to make $D_e(Ag_2)$ equal to the experimental value, VWN and PVS energies become very similar. The BLAP functional does not seem reliable for predicting structures of silver clusters. It gives a diatomic Ag–Ag bond which is too long (by 0.13 Å), too soft and too weak (ω_e and D_e are both 20% smaller than experiment). For Ag_3, it is hard to compare to experiment because BLAP gives a very flat potential from which we get only a rough estimate of the short bond length (2.74 Å) and angle (116°). For Ag_4, the BLAP relative energies of isomers (see Table VI) are at odds with calculations of Bonačić-Koutecký and co-workers[34] which strongly indicate the rhombus as the most stable structure. Nearest-neighbor interatomic distances generally increase with cluster size. For clusters with ten atoms and more, BLAP gives an average nearest-neighbor distance of about 3.00 Å, already larger than the experimental bulk interatomic distance (2.89 Å). We did BLAP calculations for many isomers not listed in Table VI. The calculated BLAP relative energies (eV) for these isomers are as follows: 9.1 $=0.02$, 9.2$=0.10$, 9.3$=0.11$, 9.4$=0.06$, and 9.5$=0.00$; 10.1$=0.08$, 10.2$=0.10$, 10.3$=0.13$, 10.4$=0.00$, 10.6 $=0.71$, 10.11$=0.73$, 10.12$=0.62$, and 10.13$=0.68$; 11.1 $=0.00$, 11.2$=0.02$, 11.3$=0.26$, 11.6$=0.63$, and 11.7 $=0.97$; and 12.1$=0.00$, 12.2$=0.15$, and 12.3$=0.04$. Predictions from BP86 and BLAP calculations regarding structures likely to have a low energy generally agree with VWN. However, the BP86 and BLAP relative energies of planar isomers are smaller by 0.2 to 0.5 eV compared to VWN. The BLAP results differ from VWN in other ways. Most bonds are longer by 0.2 to 0.4 Å compared to VWN, and isomers tend to be closer in energy in BLAP than in VWN. The BP86 optimized structures and relative energies are intermediate between those of BLAP and VWN.

The energetic trends displayed for VWN in Fig. 3 are found to be almost identical with PVS, and qualitatively

similar with BP86 and BLAP. Even-odd energy oscillations are found with all functionals, but they are slightly stronger with BLAP. We shifted the Ag atom energies for PVS and BLAP, as we did for VWN, so that the binding energy of Ag_2 matches the experiment (1.66 eV). For BP86, there is no need for an energy shift because the calculated Ag_2 binding energy (1.65 eV) is already essentially equal to the experimental value. These corrected energies are used for comparing the size dependence of energies of various functionals. The BLAP cohesive energy differs from that of other functionals. It does not increase smoothly with size, it has a maximum for planar Ag_6(1.09 eV/atom), and it is only 1.06 eV/atom for Ag_{12}. We can extrapolate cluster energies to get rough estimates of the bulk cohesive energy E_c for each functional in the following way. First, we take the ratio of the empirical SSAC cohesive energies for the bulk and for Ag_n, for $n=8$, the ratio is 1.746. Then we multiply the Ag_8 cluster cohesive energy by 1.746 to get estimates of E_c which are, in eV/atom, 3.11 (VWN), 3.07 (PVS), 2.41 (BP86), and 1.85 (BLAP). The experimental E_c for silver is 2.95 eV/atom. If we use $n=9$, 10, 11, or 12 instead, VWN gives E_c estimates that are close to one another and are in slightly better agreement with experiment (2.96, 3.02, 3.00, and 3.06, respectively), while BLAP estimates become worse (1.70, 1.71, 1.65, and 1.68, respectively). These numbers suggest that a simple shift of atomic energies improves cohesive energies obtained with VWN and PVS functionals, but does not improve energies obtained with the gradient-corrected functionals BP86 and BLAP. Note that all calculations were done with a model core potential optimized for the VWN exchange-correlation functional. Results could be slightly different if we used model core potentials and basis sets optimized separately for each functional. But our tentative conclusions regarding silver cluster energies and structures are that PVS gives results similar to VWN, BP86 generally does not seem as reliable as VWN or PVS even though it yields the Ag_2 binding energy closest to experiment, and the BLAP functional seems the least reliable.

VII. CONCLUSION

On the basis of VWN energies, and IP's compared to experiment, we tentatively assign the structure of Ag_{10} to 10.1 and Ag_{11} to 11.1; either 8.1 or 8.2, or both, are possible for Ag_8, and there are three possibilities for the structure of Ag_{12}, 12.1, 12.2, and 12.3. Ten isomers of Ag_9 have comparable VWN energies, and IP's that are either too high or too low compared to experiment. We believe that a mixture of isomers of Ag_9 is formed in experiments.

It is interesting that the least stable cluster, Ag_9, is the one with the largest number of possible isomers. We rationalize this as follows: The lowest energy isomers of silver clusters are those that simultaneously fulfill to a high degree many requirements (large γ, small δ, EJM shape, may be high symmetry). For certain sizes, there is not a single structure that meets all these requirements. When this happens, first that cluster size appears relatively unstable, and second, there are many ways to meet some, but not all, requirements for structural stability and, correspondingly, several isomers with near equal energies. In other words, when a cluster size appears unstable relative to others, it points to the possibility of multiple isomers being present.

The picture that comes out of KS-DFT calculations is that silver clusters, Ag_9 excepted, adopt one or a few specific structures at low temperature. However, silver clusters can appear as if they were liquid metal droplets for a number of reasons. First, the favored isomers have shapes that do conform with EJM predictions. This is not a coincidence. Molecular orbitals in Ag_n are delocalized, and everything else being equal, clusters adopt shapes predicted by the EJM. Second, the lowest harmonic frequencies are quite small which implies large vibrational amplitudes. Third, there are most likely two or three isomers at $n=8$ and 12, and the presence of multiple isomers becomes more likely with increasing size. Clusters like Ag_9, with many isomers, could behave as a liquid droplet if atoms can exchange places by successive isomer interconversions. It would be interesting to have measurements of the temperature dependence of properties of Ag_9 and molecular dynamics simulations to determine an effective melting temperature for Ag_9.

ACKNOWLEDGMENTS

The author thanks Nan Jiang for providing the eHMO code, and Wai-To Chan, Benoit Simard, and Steve Mitchell for valuable discussions. Yasaman Soudagar and Joey Cheng are also thanked for help with some of the calculations. This work was supported by the Natural Sciences and Engineering Research Council of Canada and by Research Corporation.

[1] J. B. Griffin and P. B. Armentrout, J. Chem. Phys. **108**, 8062 (1998); **108**, 8075 (1998).
[2] V. A. Spassov, T.-H. Lee, and K. M. Ervin, J. Chem. Phys. **112**, 1713 (2000).
[3] S. Lee, N. G. Gotts, G. von Helden, and M. T. Bowers, J. Phys. Chem. A **101**, 2096 (1997).
[4] J. Lerme, Ph. Dugourd, R. R. Hudgins, and M. F. Jarrold, Chem. Phys. Lett. **304**, 19 (1999).
[5] I. Rata, A. A. Shvartsburg, M. Horoi, T. Frauenheim, K. W. M. Siu, and K. A. Jackson, Phys. Rev. Lett. (2001) (in press).
[6] J. Conceicao, R. T. Laaksonen, L.-S. Wang, T. Guo, P. Nordlander, and R. E. Smalley, Phys. Rev. B **51**, 4668 (1995).
[7] G. M. Koretsky and M. B. Knickelbein, J. Chem. Phys. **106**, 9810 (1997).
[8] H. Kietzmann, J. Morenzin, P. S. Bechthold, G. Ganteför, and W. Eberhardt, J. Chem. Phys. **109**, 2275 (1998).
[9] J. Akola, M. Manninen, H. Häkkinen, U. Landman, X. Li, and L.-S. Wang, Phys. Rev. B **60**, 11297 (1999).
[10] A. J. Cox, J. G. Louderback, and L. A. Bloomfield, Phys. Rev. Lett. **71**, 923 (1993).
[11] R. J. Van Zee and W. Weltner, Jr., J. Chem. Phys. **92**, 6976 (1990).
[12] D. M. Rayner, K. Athenassenas, B. A. Collings, S. A. Mitchell, and P. A. Hackett, in *Theory of Atomic and Molecular Clusters with a Glimpse at Experiments*, Springer Series in Cluster Physics, edited by J. Jellinek (Springer, New York, 1999), pp. 371–395, and references therein.
[13] H. Wang, T. Craig, H. Haouari, Y. Liu, J. R. Lombardi, and D. M. Lindsay, J. Chem. Phys. **103**, 9527 (1995).
[14] E. C. Honea, A. Ogura, D. R. Peale *et al.*, J. Chem. Phys. **110**, 12161 (1999).
[15] G. M. Koretsky and M. B. Knickelbein, J. Chem. Phys. **107**, 10555 (1997).
[16] M. B. Knickelbein and G. M. Koretsky, J. Phys. Chem. A **102**, 580 (1998).
[17] D. S. Yang, M. Z. Zgierski, and P. A. Hackett, J. Chem. Phys. **108**, 3591 (1998).
[18] S. F. Cartier, B. D. May, and A. W. Castleman, Jr., J. Phys. Chem. **100**, 8175 (1996).

[19] A. Bercés, P. A. Hackett, L. Lian, S. A. Mitchell, and D. M. Rayner, J. Chem. Phys. **108**, 5476 (1998).
[20] M. B. Knickelbein, Annu. Rev. Phys. Chem. **50**, 79 (1999), and references therein.
[21] S. J. Riley, Ber. Bunsenges. Phys. Chem. **96**, 1104 (1992).
[22] P. W. Fowler and D. E. Manolopoulos, *An Atlas of Fullerenes*, International Series of Monographs on Chemistry, Vol. 30 (Clarendon, Oxford, 1995).
[23] G. von Helden, M. T. Hsu, P. R. Kemper, and M. T. Bowers, J. Chem. Phys. **95**, 3835 (1991); G. von Helden, M. T. Hsu, N. G. Gotts, and M. T. Bowers, J. Phys. Chem. **97**, 8182 (1993); K. B. Shelimov, J. M. Hunter, and M. F. Jarrold, Int. J. Mass Spectrom. Ion Processes **138**, 17 (1994).
[24] H. Kietzmann, J. Morenzin, P. S. Bechthold *et al.*, Phys. Rev. Lett. **77**, 4528 (1996).
[25] S. J. Riley, J. Non-Cryst. Solids **205/207**, 781 (1996).
[26] E. K. Parks, L. Zhu, J. Ho, and S. J. Riley, J. Chem. Phys. **100**, 7206 (1994); **102**, 7377 (1995); E. K. Parks and S. J. Riley, Z. Phys. D: At., Mol. Clusters **33**, 59 (1995).
[27] See, for example, A. A. Shvartsburg, B. Liu, Z.-Y. Liu, C.-Z. Wang, M. F. Jarrold, and K.-M. Ho, Phys. Rev. Lett. **83**, 2167 (1999).
[28] R. S. Eachus, A. P. Marchetti, and A. A. Muenter, Annu. Rev. Phys. Chem. **50**, 117 (1999).
[29] S.-H. Kim, G. Medeiros-Ribeiro, D. A. A. Ohlberg, R. Stanley Williams, and J. R. Heath, J. Phys. Chem. **103**, 10341 (1999).
[30] W.-T. Chan and R. Fournier, Chem. Phys. Lett. **315**, 257 (1999).
[31] J. Yoon, K. S. Kim, and K. K. Baeck, J. Chem. Phys. **112**, 9335 (2000).
[32] F. Wallimann, H.-M. Frey, S. Leutwyler, and M. Riley, Z. Phys. D: At., Mol. Clusters **40**, 30 (1997).
[33] E. E. Wedum, E. R. Grant, P. Y. Cheng, K. F. Willey, and M. A. Duncan, J. Chem. Phys. **100**, 6312 (1994).
[34] V. Bonačić-Koutecký, J. Pittner, M. Boiron, and P. Fantucci, J. Chem. Phys. **110**, 3876 (1999).
[35] T. L. Haslett, K. A. Bosnick, and M. Moskovits, J. Chem. Phys. **108**, 3453 (1998).
[36] K. A. Bosnick, T. L. Haslett, S. Fedrigo, M. Moskovits, W.-T. Chan, and R. Fournier, J. Chem. Phys. **111**, 8867 (1999).
[37] S. B. H. Bach, D. A. Garland, R. J. Van Zee, and W. Weltner, Jr., J. Chem. Phys. **87**, 869 (1987).
[38] R. Arratia-Pérez, L. Hernández-Acevedo, and L. Alvarez-Thon, J. Chem. Phys. **108**, 5795 (1998).
[39] V. Bonačić-Koutecký, L. Češpiva, P. Fantucci, and J. Koutecký, J. Chem. Phys. **98**, 7981 (1993).
[40] D. Bonatsos, N. Karoussos, P. P. Raychev, R. P. Roussev, and P. A. Terziev, Chem. Phys. Lett. **302**, 392 (1999), and references therein.
[41] W. A. DeHeer, Rev. Mod. Phys. **65**, 611 (1993); M. Brack, Rev. Mod. Phys. **65**, 677 (1993), and references therein.
[42] R. S. Berry, T. L. Beck, H. L. Davis, and J. Jellinek, Adv. Chem. Phys. **70**, 75 (1988).
[43] See, for example, F. H. Stillinger and T. A. Weber, Phys. Rev. B **31**, 5262 (1985).
[44] A. St-Amant and D. R. Salahub, Chem. Phys. Lett. **169**, 387 (1990); A. St-Amant, Ph.D. thesis, University of Montreal (1992); M. E. Casida, C. Daul, A. Goursot *et al.*, deMon-KS version 3.2 (deMon Software, 1998).
[45] J. Andzelm, E. Radzio, and D. R. Salahub, J. Chem. Phys. **83**, 4573 (1985).
[46] S. H. Vosko, L. Wilk, and M. Nusair, Can. J. Phys. **58**, 1200 (1980).
[47] J. P. Perdew, S. Kurth, A. Zupan, and P. Blaha, Phys. Rev. Lett. **82**, 2544 (1999).
[48] S. Yanagisawa, T. Tsuneda, and K. Hirao, J. Chem. Phys. **112**, 545 (2000).
[49] C. J. Barden, J. C. Rienstra-Kiracofe, and H. F. Schaefer III, J. Chem. Phys. **113**, 690 (2000).
[50] B. Simard, P. A. Hackett, A. M. James, and P. R. R. Langridge-Smith, Chem. Phys. Lett. **186**, 415 (1991).
[51] K. P. Huber, and G. Herzberg, *Molecular Spectra and Molecular Structure*, Constants of Diatomic Molecules, Vol. IV (Van Nostrand, Toronto, 1979).
[52] R. Fournier, S. B. Sinnott, and A. E. DePristo, J. Chem. Phys. **97**, 4149 (1992); *erratum*, *ibid.* **98**, 9222 (1993).
[53] L. A. Curtiss, P. W. Deutsch, and K. Raghavachari, J. Chem. Phys. **96**, 6868 (1992).
[54] Q. Ran, R. W. Schmude, K. A. Gingerich, D. W. Whilwhite, and J. E. Kincade, J. Phys. Chem. **97**, 8535 (1993).
[55] P. Y. Cheng and M. A. Duncan, Chem. Phys. Lett. **152**, 341 (1988).
[56] A. M. Ellis, E. S. J. Robles, and T. A. Miller, Chem. Phys. Lett. **201**, 132 (1993).
[57] S. Fedrigo, W. Harbich, and J. Buttet, J. Chem. Phys. **99**, 5712 (1993).
[58] J. P. Bravo-Vásquez and R. Arratia-Pérez, J. Phys. Chem. **98**, 5627 (1994).
[59] T. Okazaki, Y. Saito, A. Kasuya, and Y. Nishina, J. Chem. Phys. **104**, 812 (1996).
[60] D. W. Boo, Y. Ozaki, L. H. Andersen, and W. C. Lineberger, J. Phys. Chem. A **101**, 6688 (1997).
[61] T. Leisner, S. Vajda, S. Wolf, L. Wöste, and R. S. Berry, J. Chem. Phys. **111**, 1017 (1999).
[62] I. Rabin, W. Schulze, G. Ertl, C. Felix, C. Sieber, W. Harbich, and J. Buttet, Chem. Phys. Lett. **320**, 59 (2000).
[63] W. Schulze, H. U. Becker, R. Minkwitz, and K. Manzel, Chem. Phys. Lett. **55**, 59 (1978).
[64] U. Kettler, P. S. Bechthold, and W. Krasser, Surf. Sci. **156**, 867 (1985).
[65] S. Krückeberg, G. Dietrich, K. Lützenkirchen, L. Schweikhard, C. Walther, and J. Ziegler, J. Chem. Phys. **110**, 7216 (1999).
[66] V. A. Spasov, T. H. Lee, J. P. Maberry, and K. M. Ervin, J. Chem. Phys. **110**, 5208 (1999).
[67] Y. Shi, V. A. Spasov, and K. M. Ervin, J. Chem. Phys. **111**, 938 (1999).
[68] G. Alameddin, J. Hunter, D. Cameron, and M. M. Kappes, Chem. Phys. Lett. **192**, 122 (1992).
[69] C. Jackschath, I. Rabin, and W. Schulze, Z. Phys. D: At., Mol. Clusters **22**, 517 (1992).
[70] J. Ho, K. M. Ervin, and W. C. Lineberger, J. Chem. Phys. **93**, 6987 (1990).
[71] G. Ganteför, M. Gausa, K.-H. Meiwes-Broer, and H. O. Lutz, J. Chem. Soc., Faraday Trans. **86**, 2483 (1990).
[72] K. J. Taylor, C. L. Pettiette-Hall, O. Cheshnovsky, and R. E. Smalley, J. Chem. Phys. **96**, 3319 (1992).
[73] H. Handschuh, C.-Y. Cha, H. Möller, P. S. Bechthold, G. Ganteför, and W. Eberhardt, Chem. Phys. Lett. **227**, 496 (1994).
[74] H. Handschuh, C.-Y. Cha, P. S. Bechthold, G. Ganteför, and W. Eberhardt, J. Chem. Phys. **102**, 6406 (1995).
[75] L. Lian, S. A. Mitchell, P. A. Hackett, and D. M. Rayner, J. Chem. Phys. **104**, 5338 (1996).
[76] S. Fedrigo, W. Harbich, and J. Buttet, Phys. Rev. B **47**, 10706 (1993).
[77] I. Rabin, W. Schulze, and G. Ertl, Chem. Phys. Lett. **312**, 394 (1999).
[78] B. A. Collings, K. Athanassenas, D. M. Rayner, and P. A. Hackett, Chem. Phys. Lett. **227**, 490 (1994).
[79] J. Tiggesbäumker, L. Köller, H. O. Lutz, and K. H. Meiwes-Broer, Chem. Phys. Lett. **190**, 42 (1992).
[80] J. Lermé, B. Palpant, B. Prével, M. Pellarin, M. Treilleux, J. L. Vialle, A. Perez, and M. Broyer, Phys. Rev. Lett. **80**, 5105 (1998).
[81] B. Palpant, H. Portales, L. Saviot, *et al.*, Phys. Rev. B **60**, 17107 (1999).
[82] V. Bonačić-Koutecký, L. Češpiva, P. Fantucci, J. Pittner, and J. Koutecký, J. Chem. Phys. **100**, 490 (1994).
[83] H. Deutsch, J. Pittner, V. Bonačić-Koutecký, K. Becker, S. Matt, and T. D. Märk, J. Chem. Phys. **111**, 1964 (1999).
[84] D. A. McQuarrie, *Statistical Mechanics* (Harper & Row, New York, 1976) p. 156, Eqs. (9–62).
[85] G. A. Arteca, Rev. Comput. Chem. **9**, 191 (1996).
[86] L. L. Lohr and W. N. Lipscomb, J. Chem. Phys. **38**, 1607 (1963); R. Hoffmann, J. Chem. Phys. **39**, 1397 (1963); M. C. Zerner, Rev. Comput. Chem. **2**, 313 (1991).
[87] M. Methfessel, D. Hennig, and M. Scheffler, Appl. Phys. A: Solids Surf. **55**, 442 (1992).
[88] A. D. Becke, Phys. Rev. A **38**, 3098 (1988).
[89] J. P. Perdew, Phys. Rev. B **33**, 8822 (1986).
[90] E. I. Proynov and D. R. Salahub, Phys. Rev. B **49**, 7874 (1994), and *erratum*, *ibid.* **57**, 12616 (1998); E. Proynov, A. Vela, and D. R. Salahub, Chem. Phys. Lett. **230**, 419 (1994), and *erratum*, *ibid.* **234**, 462 (1995); E. I. Proynov, E. Ruiz, A. Vela, and D. R. Salahub, Int. J. Quantum Chem. **29**, 61 (1995); E. I. Proynov, S. Sirois, and D. R. Salahub, Int. J. Quantum Chem. **64**, 427 (1997).
[91] E. I. Proynov, A. Vela, and D. R. Salahub, Phys. Rev. A **50**, 3766 (1994).
[92] Y. Soudagar and R. Fournier (unpublished).